*J Toxicol Pathol 2009; **22**: 273–279*

Original

Skeletal Muscle for Endomyocardial Biopsy: Comparable Stress Response in Doxorubicin Cardio-myopathy

Rosa Maita[1], Mirian Strauss[1], and Guillermo Anselmi[1]

[1]Sección de Biología Celular, Instituto de Medicina Tropical, Facultad de Medicina, Universidad Central de Venezuela, Caracas, Venezuela

Abstract: In the present study, we compared the cell damage response in skeletal and cardiac muscle tissue when exposed to doxorubicin. This was carried out by means of a less invasive informative substitute to endomyocardiac biopsy based on Hsp70 immunodetection and a subcellular analysis of the nucleolus. Male Sprague Dawley rats (62 g body weight) were randomly distributed into 3 group, the control and doxorubicin I and doxorubicin II groups, in which 15 and 25 mg/kg body weight of doxorubicin (0.1 ml, i.v.) was administered, respectively. After 15, 30, 45 and 60 minutes, portions of the left and right ventricle wall and interventricle wall, together with skeletal muscle from the posterior and anterior member, were prepared for Hsp70 immunodetection by Western blot analysis and ultrastructural study using the thin cut technique. Differential cell response between the control and treated groups was observed in Hsp70 immunodetection and at the subcellular level. In the control group, the Hsp70 recognition levels and typical normal nucleolar morphology were similar, while the treated groups showed variable-dependent Hsp70 recognition and segregation of nucleolar components, forming ring-like figures of a variable-independent nature. Comparison of cardiac and skeletal muscle tissue cell response to doxorubicin toxic aggression revealed parallelism in terms of Hsp70 accumulation in certain regions of both tissues (15 mg/kg body weight of doxorubicin), which suggests that replacing endomyocardiac biopsy analysis with skeletal muscle analysis may be a safe option. (J Toxicol Pathol 2009; **22**: 273–279)

Key words: doxorubicin, endomyocardiac biopsy, nucleolar segregation, muscle skeletal biopsy, Hsp70

Introduction

Clinical use of anthracyclines can be viewed as a sort of double-edged sword. The anthracyclines, including doxorubicin (DOX), play an undisputed, key role in the treatment of many neoplastic diseases, but they also cause cardiotoxicity and/or introduce a measurable risk of delayed cardiovascular events[1–3]. In addition, the ultrastructural features of anthracycline-induced cardiomyopathy, evidenced in patients' endomyocardial biopsies, are also seen in mice, rats and rabbits treated with the drug, indicating the existence of species-independent morphologic damage[4]. Despite the side effects, DOX is considered irreplaceable and as a result is widely employed[5,6]. Currently, the most common method used to detect anthracycline-induced cardiotoxicity is evaluation of functional parameters, including the left ventricular ejection fraction and fractional shortening by echocardiography[7]. However, serious, irreversible heart damage must occur for these tests to be considered abnormal[8]. In this regard, detection of anthracycline-induced cardiotoxicity at an early stage is still disputed. Endomyocardial biopsy (EMB) remains the golden standard with which to assess and diagnose myocardial disease in patients[9]. However, its invasive characteristic, given the clinical importance of myocardiac damage caused by DOX, represents an additional element of aggression for the pathological cardiac condition, which limits its usefulness[10]. Given the risks of using EMB, it is necessary to seek a less invasive alternative or one that is non-invasive, safe, accurate, informative and predictive with respect to the cardiac condition and yet capable of preserving antineoplasic effectiveness. The similarity between heart and skeletal muscle at the ultrastructural level after DOX treatment has previously been pointed out by Meski *et al.*[11] Moreover, the stress-dependent changes in nucleolar reorganization are associated with cell response to the proteotoxic damage resulting from elevated expression of heat-shock proteins (Hsps) that function as molecular chaperones and maintain vital homeostasis of the protein folds. In this regard, when subjected to stress there is a tissue-specific Hsp70 response in animals[12]. The differential expression of Hsp70 and

Received: 24 June 2009, Accepted: 17 July 2009
Mailing address: Mirian Strauss, Sección de Biología Celular, Instituto de Medicina Tropical, Universidad Central de Venezuela, Apartado Postal 47019, Caracas 1041-A, Venezuela
TEL: 58-212-6053650 FAX: 58-212-2434685
E-mail: mstraussve@gmail.com

ultrastructural features in heart and liver rat tissue after short-term DOX treatment have previously been shown[13], which means that they can now be used as comparative indicators of the degree of susceptibility in tissue submitted to similar toxic aggression. On the other hand, a reduction of Hsp70 expression in rat cardiac muscle after chronic DOX treatment has been demonstrated[14]. In this work, we investigated the Hsp stress response in cardiac and skeletal tissue induced by DOX toxic aggression. Principally, we examined the expression of Hsp70 in the right and left ventricular free walls, interventricular septum and anterior and posterior skeletal limb muscle plus the changes in nucleolar reorganization of all regions at two DOX dosages and four different post-treatment times. Cardiac, versus skeletal, tissue cell response to DOX toxic aggression reveals parallelism in terms of Hsp70 expression and the relationship to nucleolar reorganization. In this regard, substitution of one tissue for another based upon cellular similarity stress response would be advantageous since it could prevent additional damage to the heart, while providing information about cell response to antineoplastic treatment. Skeletal muscle biopsy represents a possible informative substitute for EMB in DOX cardiomyopathy.

Methods

Animals

Male Sprague Dawley rats (body weight 62 ± 5 g; 3–4 weeks of age) were acquired from the Instituto Venezolano de Investigaciones Científicas (Caracas, Venezuela). The rats were allowed free access to a standard diet and water *ad libitum*. This investigation complied with the norms set out in the Guide for the Care and Use of Laboratory Animals published by the US National Institutes of Health (NIH publication No. 85–23, revised 1996) and related ethical regulations of the Universidad Central de Venezuela , Instituto de Medicina Tropical.

Materials

DOX, monoclonal anti-heat shock protein 70 (Hsp70, clone BRM-22) and anti-mouse IgG peroxidase conjugate were obtained from Sigma-Aldrich (St. Louis, MO, USA). Chemiluminescent substrate from Pierce Biotechnology (Rockford, IL, USA). Bio-Rad Laboratories (Hercules, CA, USA) was the source of all other biochemical compounds. The components used in the ultrastructural study were obtained from Electron Microscopy Sciences (Hatfield, PA, USA).

DOX administration protocol

Rats were randomly distributed into three groups (12 each): Control group (CON), Doxorubicin I (DOX-I) and Doxorubicin II (DOX-II). DOX was administered in single doses of 15 or 25 mg/kg (0.1 ml, i.v.) body weight, respectively. The selection of DOX dosage was base on unpublished data from a previous study in our laboratory of LD_{100}, which is defined as the lethal dose required to cause death in 100% of rats within 24 and 48 hours. The CON group rats received sterile water (0.1 ml; i.v.). After 15, 30, 45 and 60 minutes post-treatment of the animals (3 each), the left and right ventricular and interventricular walls (LV, RV and IV, respectively) and posterior (medial head of gastronemius) and anterior (extensor carpi ulnaris) member skeletal muscle (PM and AM, respectively) were removed for subsequent analysis.

Ultrastructural analysis

The samples from both muscle tissues were fixed with Karnovsky's fixative (320 mosmol, pH 7.4, for 2 h, at 4°C), post-fixed in osmic acid (osmium tetroxide, 2% 0.12 M 2 h 4°C 320 mosmol, pH 7.4) dissolved in phosphate buffer (l h at room temperature) and dehydrated in acetone (50%, 70%, 80%, 95% and 100%; 30 min each). Finally, they were embedded in epoxy resin (60°C, 48 h). After embedding, thin sections were cut (Reichert OM-U3 ultramicrotome), stained with saturated uranyl acetate (45 min, 60°C, moist chamber) and lead citrate (15 min, room temperature, dry chamber) and examined with a transmission electron microscope (Hitachi 300, 70 kvol).

Western blot analysis

The samples from both muscle tissues were homogenised (4°C; 1 ml extraction buffer composed of 20 mM Tris-HCL, 2 mM EDTA and 1mM PMSF, pH 7.4) using a Potter-Elvehjem tissue grinder. The samples were centrifuged (14.000 RPM/10 min, 4°C), and the pellet was discarded. The protein content in the resulting supernatants was determined by Bradford microassay[15] using albumin as a standard. Equal amount of proteins (3.6 μg) diluted in a 4× SDS sample buffer (10 mM tris-HCL, pH 6.8; 1% SDS, 1% 2-β-mercaptoethanol, 1% glycerol, a small amount of bromophenol blue and pyronin) were separated on 10% polyacrylamide gels by SDS-PAGE[16] in duplicated gels. One of the gels was stained with Coomassie Brilliant Blue G-250 to confirm the equivalence of the loading concentrations and adequacy of sample preparation, while a second gel was transferred to a nitrocellulose membrane and stained with Ponceau Red before inmunobloting[17]. Nonspecific binding sites of the membranes were blocked (0.1% Tween 20 and 5% non-fat milk in PBS, pH 7.4), incubated with the primary monoclonal anti-Hsp70 antibody (1:5000) and then incubated with the secondary horseradish peroxidase-conjugated-rabbit anti mouse IgG antibody (1:4000). The washes were performed with 0.1% Tween 20 in PBS (pH 7.4). Inmunoreactive bands were revealed by a chemoluminescent substrate and exposed to Kodak X-ray film for 2 minutes. The relative levels of the protein bands were determined using an optical densitometry (GS-800 Densitometer and Quantity One software, Bio-Rad Laboratories).

Statistical analysis

Data are expressed as means ± SEM of at least three

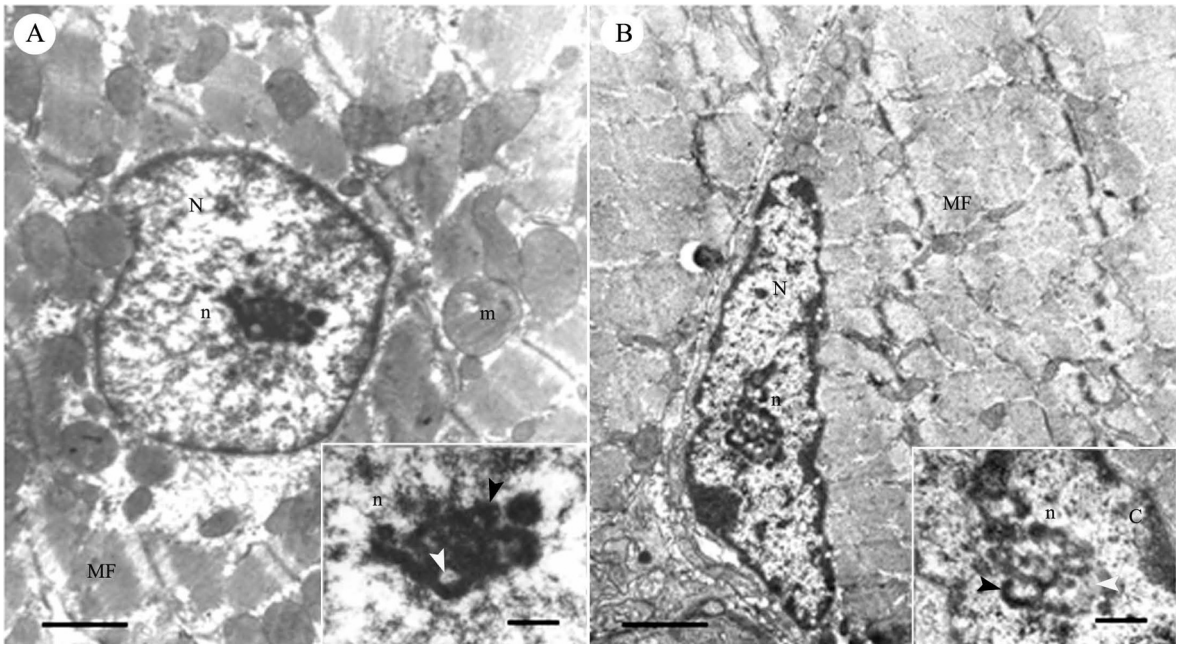

Fig. 1. Transmission electron micrographs of a cardiac muscle (A) and skeletal muscle cells (B) from the control group. Characteristic central and peripheral positions of the nuclelus and a typical distribution of nucleolar components (inset) was observed Nuclei (N), Nucleolus (n), nucleolar organisation region (white arrow head) and the granular component (black arrow head). Myofibrils (MF), mitochondria (m) and the perinuclear chromatin (C) were also revealed. Scale bars: 1 μm (Figs. 1A, 1B) and 0.12 μm (insets, taken at 75 kV).

independent experiments. Non-normal distribution, Kruskal-Wallis and Mann-Whitney U tests were used. All tests performed were two-sided, and statistical significance was defined as $P<0.05$. All statistical analyses were performed using SPSS Statistics for Windows 17.0 (SPSS, Inc., Chicago, IL, USA).

Results

Ultrastructural analyses

A concentric accumulation of macromolecules in random distribution, typical of a cell under normal conditions, was observed in the nucleolus of both muscle types from the CON group, where a region of nucleolar organisation (RNO) and a dense fibril and granular component (DFC and GC, respectively; Fig. 1) were identified. In contrast, in the DOX-I and DOX-II groups, a tendency towards segregation of components or compact nucleolar structures was observed for all DOX post-treatment times (Figs. 2, 3). In the nucleoli of cardiac tissue (A–D, Figs. 1, 2) and skeletal muscle tissue (E–H, Figs. 1, 2), the segregation was characterised principally by a ring-like configuration, with a less electron-dense element in a central or lateral location (Fig. 2, A–D, E, H; Fig. 3, A–D, F). The compact nucleolar structures evidenced a tight grouping of electron-dense elements in a spherical shape, in which an accumulation of less electron-dense elements, often towards the periphery, could also be observed (Fig. 2, F–G; Fig. 3, E, G, H).

Hsp70 immunodetection

Hsp70 recognition in the CON group was similar in the LV, RV, IV and PM, but was slightly less in the AM (Figs. 4, 5). In contrast, in the DOX-I group, two similar patterns of Hsp70 recognition were evident among the regions and tissues. One pattern, in the LV, RV and PM, was related to greater Hsp70 recognition, while the other in the IV and AM, was related to lesser Hsp70 recognition. The difference between these two patterns was statistically significant ($p<0.05$, Kruskal-Wallis and Mann-Whitney U test). In addition, greater recognition was also evidenced in all muscle zones. Recognition was greater at 45 min compared with 15 and 60 min, respectively. At 30 min, recognition was noticeably less (Figs. 4, 5).

This differential recognition was statistically significant ($p<0.05$, Kruskal-Wallis and Mann-Whitney U test).

Compared with the DOX-II group, tissue and time-independent Hsp70 recognition was clearly evidenced in a uniform zone, similar to the CON group, although detection in the latter was slightly greater. Differential Hsp70 recognition was only observed at 60 min and was characterized as being greater in the LV and IV than in the RV, AM and PM ($p<0.05$, Kruskal-Wallis and Mann-Whitney U test, Figs. 4, 5).

Discussion

The similarity in nucleolar alterations observed in the two types of tissue exposed to DOX corresponds to the

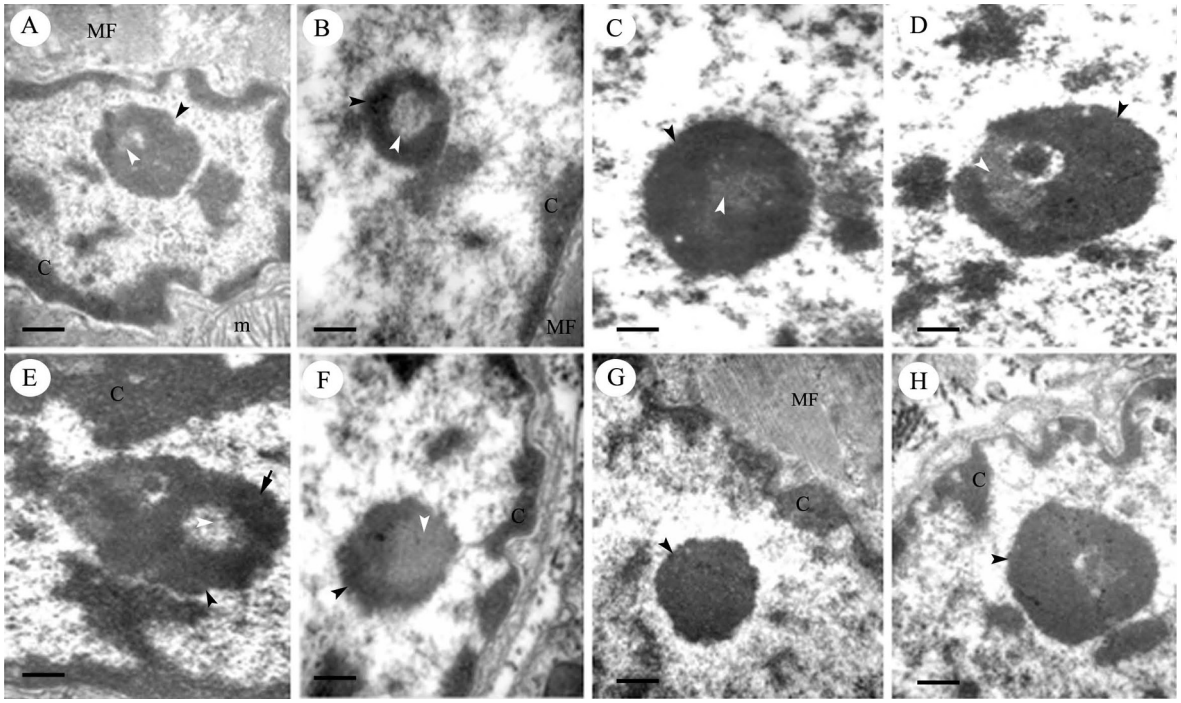

Fig. 2. Transmission electron micrograph of cardiac muscle and skeletal muscle cell nucleoli with respect to different post-treatment times of a low dose of doxorubicin (DOX-I group: 15 mg/kg bw). The reorganisation of nucleolar components showed segregation of nucleolar components (A–D, E, H) and compact nucleorar structures (F–G). Cardiac muscle cells (A–D), skeletal muscle cells (E–H). Post-treatment times (in minutes): 15 (A, E), 30 (B, F), 45 (C, G), 60 (D, H). Nucleolar organisation region (white arrow head), dense fibrilar component (arrow), granular component (black arrow head); myofibrils (MF), mitochondria (m) and perinuclear chromatin (C). Scale bar: 0.12 μm, taken at 75 kV.

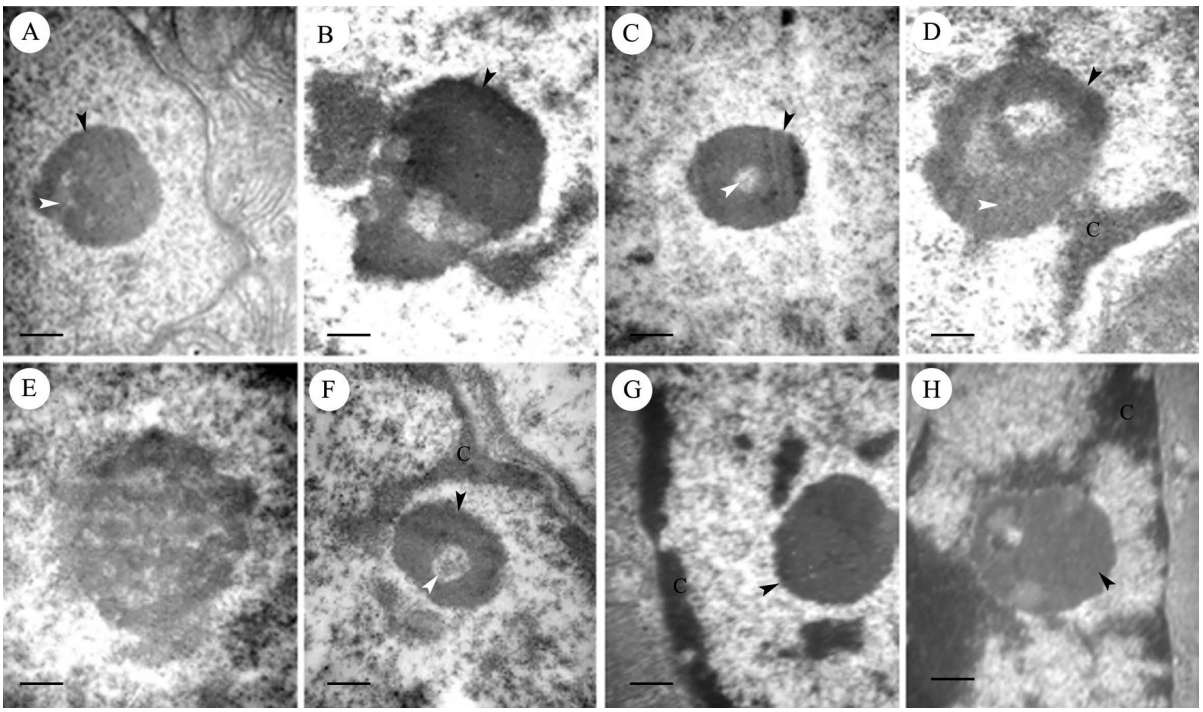

Fig. 3. Transmission electron micrograph of cardiac muscle and skeletal muscle cell nucleoli with respect to different post-treatment times of a high dose of doxorubicin (DOX-II group: 25 mg/kg bw). The reorganisation of nucleolar components showed segregation for nucleolar components (B–D, F, H), and compact nucleorar structures (A, G) were observed in all post-treatment times. Cardiac muscle cells (A–D), skeletal muscle cells (E–H). Post-treatment times (in minutes): 15 (A, E), 30 (B, F), 45 (C, G), 60 (D, H). Nucleolar organisation region (white arrow head), dense fibrilar component (arrow), granular component (black arrow head), and perinuclear chromatin (C). Scale bar: 0.12 μm, taken at 75 kV.

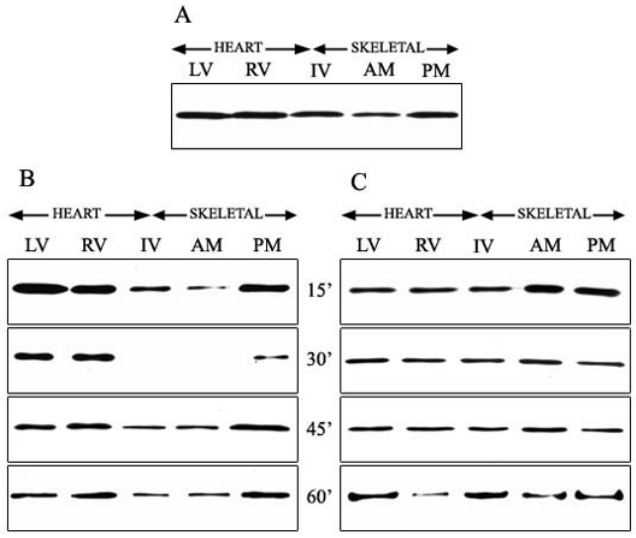

Fig. 4. Western blot analysis of Hsp 70 from the cardiac and skeletal muscle tissue of the CON and DOX groups at the post-administration times. Similar Hsp70 recognition between the LV, RV, IV and PM, slightly less recognition in the AM, were observed in the CON group. A greater amount of Hsp70 was recognized in the LV, RV and PM in the DOX-I group compared with the IV and AM, for all post-treatment times. In the DOX-II group, tissue and time independent Hsp70 recognition were observed in a uniform region for all time points except 60 min, with recognition in the LV and IV greater compared with the RV, AM and PM. A: Control group (sterile water: 0.1 ml; i.v). B: DOX-I group (15 mg/kg bw). C: DOX-II group (25 mg/kg bw. Post-treatment times (in minutes): 15, 30, 45 and 60. Tissues regions: left (LV) and right ventricular (RV) and interventricular walls (IV) and posterior (PM) and anterior member skeletal muscle (protein μg per lane: 3.6 μg).

findings of Merski *et al*. who showed the tissue-dependent nature of the event[11]. This nucleolar alteration has been identified as the morphological biomarker of cell damage[18–20] and has been linked to the process of translocation and subsequent accumulation of members of the Hsp70 family in the nucleus as a result of stress[21, 22]. All the members of this family recognized by the anti-Hsp70 monoclonal mouse antibody are made up of isoforms. Under normal conditions, they are expressed constitutively, such as Hsp73 and the stress-inducible isoform Hsp72, which constitute important stress proteins located in the cytosol and nucleus of the cells of mammals. In this respect, the parallelism in recognition of Hsp70 bands observed in all the muscle zones investigated in the CON groups reflects the similarity in the content of constitutive isoforms under normal conditions. This presence under normal conditions may represent the starting point from which the cell is equipped with the capacity to respond rapidly to adverse conditions. In the DOX-I group, the zone-tissue dependent differential pattern of Hsp70 recognition for all the post-treatment times in the present study seems to be associated with different susceptibility. The susceptibility can be related to the differential expression of Hsps in function of the role of the tissues in restoration of protein homeostasis[23].

This differential response in Hsp70 recognition can only occur within the interval of homeostatic cell adaptability, during which there is certain proportionality between the degree of toxic damage and the capacity of cell response[24].

During this interval, the characteristic zone and tissue differences predominate among the range of endogenous cell protection mechanisms in the specific tissue space. These differences in terms of the intrinsic characteristics of cell

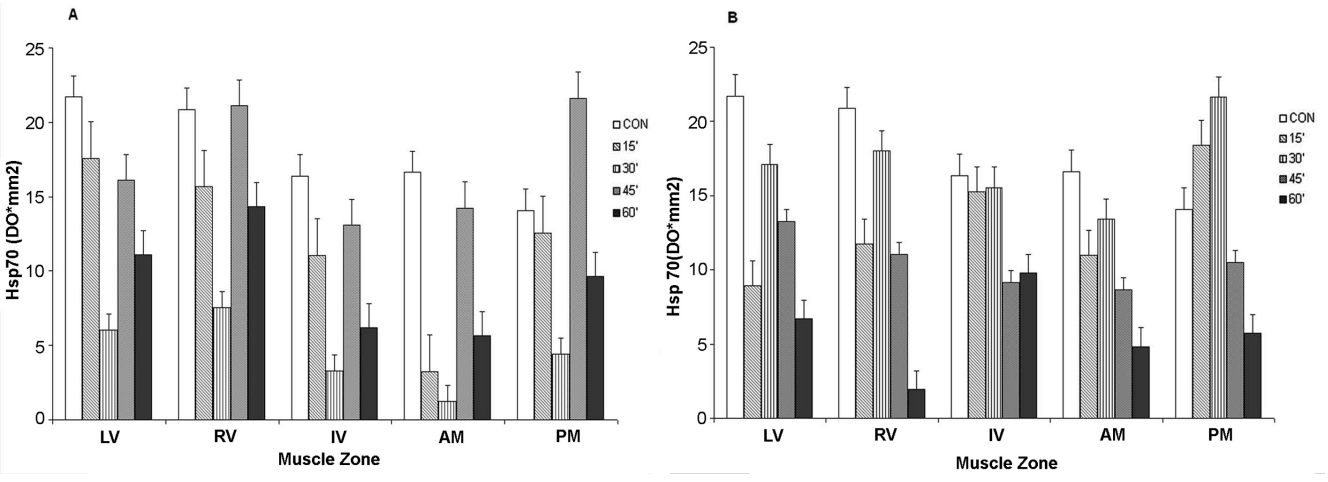

Fig. 5. Densitometric analysis of the relative levels of Hsp70 accumulation in the cardiac and skeletal tissue regions in the DOX I (A: 15 mg/kg bw) and DOX II (B: 25 mg/kg bw) groups compared with the CON (sterile water, 0.1 ml i.v.) group for the different post-treatment times (in minutes). In CON group, the accumulation of Hsp70 was similar in the LV, RV, IV and PM, with recognition slightly less in the AM. By contrast, in the DOX I group, the relative levels of Hsp70 accumulation in the LV, RV and PM were greater than in the IV and AM for all post-treatment times; in the DOX-II group, the relative levels of Hsp70 accumulation were uniform in all regions and for all post-treatment times, except at 60 min, at which the levels were greater in the LV and IV compared with the RV, AM and PM. Tissues regions: left (LV), right ventricular (RV) and interventricular walls (IV) and posterior (PM) and anterior (AM) member skeletal muscle. Data are means ± S.E. of 3 animals in each group. $P<0.05$.

types, which were outlined by Beck *et al*., are what determine the expression of heat shock genes, rather than specific physiological or environmental conditions[25]. One example of the specificity of zonal susceptibility associated with a particular tissue can be found in the work of Strauss et al., who showed a substantial reduction in the thickness of the left ventricle wall compared with the right wall after eight and twelve weeks post-DOX-treatment[26]. Besides this, the work of Oishi *et al*.[27] also showed a differential response of Hsps to heat stress in slow and fast regions of rat gastrocnemius muscle. In general, the expression of Hsp70 was reduced in both the cardiac and skeletal muscles regardless of the region after DOX treatment.

Since Hsp expression varies from one cell type to another, this tissue-dependent differential pattern in Hsp recognition suggests an apparent similarity between the LV, RV and PM on the one hand and between IV and AM on the other, in regard to cell response to toxic damage generated by the sub-lethal dosage in the DOX-I group. This pattern of similarity would in turn justify our proposal for substituting endomyocardiac biopsies with skeletal muscle biopsies. In contrast, the uniformity in the Hsp70 recongnition in the DOX-II group with respect to the distinct muscle zones analyzed for the two types of tissue could be accounted for by the displacement of cellular response capacity to the limits of the homeostatic adaptability interval[23], where cell response tends to be linear. This dosage-dependency in Hsp70 recognition in the muscle zones and time periods analysed is in line with previous findings showing that the magnitude, type and duration of response depends on the degree of damage generated by the toxic aggression, with the maximum response corresponding to the point at which Hsps are synthesized to a maximum extent[28]. The lack of an exact correspondence between the levels of cellular organization analyzed can be explained in terms of the findings reported by De Haans[29], who argued that cellular differences that are not detected at a morphological level can be identified or highlighted at the molecular level. Finally, the apparent similarity found between the cardiac and skeletal muscle should continue to be evaluated in regard to the possibility of substituting endomyocardiac biopsies for skeletal muscle analyses within the interval of homeostatic cell adaptability in response to DOX toxic aggression.

Comparison of cardiac and skeletal muscle tissue cell response to DOX toxic aggression revealed explicit similarity in terms of Hsp70 accumulation in certain regions of both tissues, which suggests that the possibility of replacing endomyocardiac biopsy analysis with skeletal muscle analysis may be a safe option.

Acknowledgements: This work was supported by LOCTI-UCV (Laboratorios Elmor S.A.) and the Consejo de Desarrollo Científico y Humanístico (CDCH) from the Universidad Central de Venezuela. The authors extend their thanks to Prof Phillip Shultz and Marianela Rodríguez for their valuable help with the English and Electron Microscopy technical support, respectively.

References

1. Doroshow JH. Doxorubicin-induced cardiac toxicity. N Engl J Med. **324**: 843– 845. 1991.
2. Minotti G, Menna P, Salvatorelli E, Cairo G, and Gianni L. Anthracyclines: Molecular advances and pharmacologic developments in antitumor activity and cardiotoxicity. Pharmacol Rev. **56**: 185–229. 2004.
3. Menna P, Salvatorrelli E, and Minotti G. Cardiotoxicity of antitumor drugs. Chem Res Toxicol. **21**: 978–989. 2008.
4. Singal PK, Li T, Kumar D, Danelisen I, and Diskovic N. Adriamycin-induced heart failure: mechanism and modulation. Mol Cell Biochem. **207**: 77–86. 2000.
5. Wang JJ, Cortes E, Sinks LF, and Holland JE. Therapeutic effect and toxicity of adriamycin in patients with neoplastic disease. Cancer. **28**: 837–843. 1971.
6. Outomuro D, Grana DR, Azzato F, and Milei J. Adriamycin-induced myocardial toxicity: new solutions for an old problem? Inter J Cardiol. **117**: 6–15. 2007.
7. Kilickap S, Barista L, Akgul E, Aytemir K, Aksoyek S, Aksoy S, Celik L, Kes S, and Tekuzman G. CTnT can be useful marker for early detection of anthracycline cardiotoxicity. Annals of Oncology. **16**: 798–804. 2005.
8. Billingham M and Bristow M. Evaluation of anthracycline cardiotoxicity: Predictive ability and functional correlation of endomyocardial biopsy. Cancer Treat Symp. **3**: 71–76. 1984.
9. Cunningham KS, Veinot JP, and Butany J. An approach to endomyocardial biopsy interpretation. J Clin Pathol. **59**: 121–129. 2006.
10. Wiklund L, Caidahl K, Kjellstrom C, Nilsson B, Svensson G, and Berglin E. Tricuspid valve insufficiency as a complication of endomyocardial biopsy. Transpl Int. **5**: S255–S558. 1992.
11. Merski JA, Daskal Y, and Busch H. Comparison of adriamycin-induced nucleolar segregation in skeletal muscle, cardiac muscle, and liver cells. Cancer Treat Rep. **62**: 771–778. 1978.
12. Flanagan SW, Ryan AJ, Gisolfi CV, and Moseley PL. Tissue-specific HSP70 response in animals undergoing heat stress. Am J Physiol. **268**: R28–R32.1995.
13. Strauss M and Porras N. Heat shock protein 70 differential expression and ultrastructural features in heart and liver after short-term adriamycin treatment: the protective role of L-carnitine. Invest Clin. 48: 33– 43. 2007.
14. Simoncikova P, Ravingerova T, and Barancik M. The effect of chronic doxorubicin treatment on mitogen-activated protein kinases and heat stress proteins in rat hearts. Physiol Res. **57**: S97–S102 . 2008
15. Bradford MMA. Rapid and sensitive method for the quantization of microgram quantities of protein utilizing the principle of dye-binding. Anal Biochem. **72**: 248–254. 1976.
16. Laemmli UK. Cleavage of structural proteins during the assembly of the head of bacteriophage T4. Nat. **227**: 680–685. 1970.
17. Towbin H, Staehelin T, and Gordon J. Electroforetic transfer of protein from polyacrilamide gels to nitrocellulose sheets: procedure and some applications. Proc Natl Acad Sci USA. **76**: 4350–4354. 1979.
18. Imazawa T, Nishikawa A, Tada M, Takahashi M, and Hayashi Y. Nucleolar segregation as an early marker for DNA damage; an experimental study in rats treated with 4-

hydroxyaminoquinoline 1-oxide. Virch Archiv. **426**: 295–300. 1995.
19. Abe T, Fukamachi Y, Kanazawa Y, Furukawa H, Shimizu K, Hirano T, Kasai H, Kashimura M, and Higashi K. Inhibition of nucleolar function and morphological change by adriamycin associated with heat shock protein 70 accumulation. Jnp J Cancer Res. **87**: 945–951. 1996.
20. Jamison JM, Gilloteaux J, Thiry M, Authelet M, Goessens G, and Summers JL. UItraestructural nucleolar alterations induced by an ametantrone-poly r (A–U) complex. Tissue & Cell. **30**: 475–484. 1998.
21. Pelham HR. Hsp70 accelerates the recovery of nucleolar morphology after heat shock. EMBO J. **3**: 3095–3100. 1984.
22. Ellis S, Killender M, and Anderson RL. Heat-induced alterations in the localization of HSP72 and HSP73 as measured by indirect immunohistochemistry and immunogold electron microscopy. J Histochem Cytochem. **48**: 321–332. 2000.
23. Santoro MG. Heat shock factors and the control of the stress response. Biochem Pharm. **59**: 55–63. 2000.
24. Trump FB and Berezesky KI. Cellular and molecular basis of toxic cell injury. In: Cardiovascular Toxicology, 2nd ed D Acosta (eds). Raven Press, New York. 75–11. 1992.
25. Beck SC, Paidas CN, Tan H, Yang J and De Maio A. Depressed expression of the inducible form of HSP 70 (Hsp 72) in brain and heart after in vivo heat shock. Am J Physiol. **269**: R608–R613. 1995.
26. Strauss M, Anselmi G, Hermoso T, and Tejero F. Carnitine promotes heat shock protein synthesis in adriamycin-induced cardiomyopathy in neonatal rat experimental model. J Mol Cell Cardiol. **30**: 2319–2325. 1998
27. Oishi Y, Taniguchi K, Matsumoto H, Ishihara A, Ohira Y, and Roy RR. Differential responses of HSPs to heat stress in slow and fast regions of rat gastrocnemius muscle. Muscle Nerv. **28**: 587–594. 2003.
28. Craig EA and Gross CA. Is hsp70 the cellular thermometer? Trends Biochem Sci. **16**: 135–140. 1991.
29. DeHaan RL. Morphogenesis of the vertebrate heart. In: Organogenesis. RL DeHaan, H Ursprung (eds). Holt Rinehart & Winston, New York. 377– 419. 1965.